High current density DC-DC converter with Modified PI controller for fast charging applications in EVs

J. Sridevi[1*], *M*. Gayatri[1], *K*. Sharada[1], *Shabana* Begum[1], *A. H.* Shnain[2]

[1]Department of EEE, Gokaraju Rangaraju Institute of Engineering and Technology, Hyderabad, Telangana, India
[2]Department of Refrigeration and air Conditioning Techniques engineering, College of technical engineering, The Islamic University, Najaf, Iraq.

Abstract. As electric vehicles (EVs) become increasingly prevalent, the demand for efficient and high-performance DC–DC converters in the charging infrastructure is paramount. Electric vehicles, powered by rechargeable batteries or fuel cells, hence is necessary to have a cost-effective and efficient battery charger to deliver the consistent output current needed for the designated EV's battery. This paper adds a new and more effective approach of design and control of a DC–DC converter with bidirectional capability appropriate for incorporation in EV charging systems aimed at enhancing the current density and control issues inherent in the charging /discharging process. It appears to provide the necessary high current density besides battery out as soon as possible and also to impose an unimportant overshooting of the charging time for demanded lithium-ion battery system while charging it. The converter circuit contains the following equipment in its construction include single phase AC voltage source, linear transformer, passive component that includes the inductor and capacitor and bridge rectifier. Usually, Simulink/MATLAB is used for the purpose of various simulations. Using the MATLAB simulation the design of the concept system offered in this proposal has been proved. Monitored the current in amperes that the battery charger is supplying to the battery, closely observed the condition and voltage of the battery.

1 Introduction

ELECTRICS charging systems are core components of electrification in electric vehicles (EVs), thus charging systems with lower costs and minimum efficiency are prerequisite to any discussion of EVs. This can is well addressed by using Ac-dc converters to charges the set up to the level required in the most efficient way. But between AC-DC converters there is still difference in terms of stress, loss power and safety even between the isolated and non-isolated type of converter as shown in the diagram. The non-isolated systems make even greater demands on the diodes and active switches and therefore, are more power hungry and

* Corresponding Author: sridevi.j.8@gmail.com

heat prone making them more dangerous. However, isolated systems are beneficial because voltage can be lowered, power losses are reduced, temperature of devices diminishing, and safety enhanced all of which culminates in providing greater reliability to multiple systems. This system employs the usage of bridge rectifier in converting AC to DC whereas correcting for issues normally rectified through conventional rectifier such as high degree of power loss, low power factor (PF), and high overall total harmonic distortion (THD). They are eliminated by putting a LIVE to LIN COMMON gate or LCL filter next to the bridge rectifier. Following this due to the lithium-ion battery's state alterations, voltage adjustments are implemented utilizing a closed-looph DC- DC converter. But the conventional closed loop converters are often had a large value of power loss with the active switches and so changes deleterious impacts on system lifetime due to switching, leakage and conduction power loss. There are also other potential issues that could arise to lithium ion battery more particularly with voltage overshoot at the battery voltage and the output current. To overcome these challenges, this paper is presenting an application of proportional integral (PI) controller, though some alteration made in to this controller. Consequently, the achievement is the maximum efficiency and perform the AC-DC conversion with a voltage as close to the lithium-ion battery charging voltage in EV's as possible, without the voltage overshoot and the power losses in the LV and HV systems.2 PROPOSED DC-DC CONVERTER

The designed converter is shown in Fig.1. It consists of single-phase input voltage source, LCL filter, bridge rectifier, RC filter, DC-DC converter, PI controller, MOSFETS. Here single-phase AC source is used to deliver power to battery. LCL filter is connected to the AC source for filtering purposes. A Bridge-Rectifier is used to obtain DC flow. To control the MOSFETS logic a PI controller (which is modified) is used.

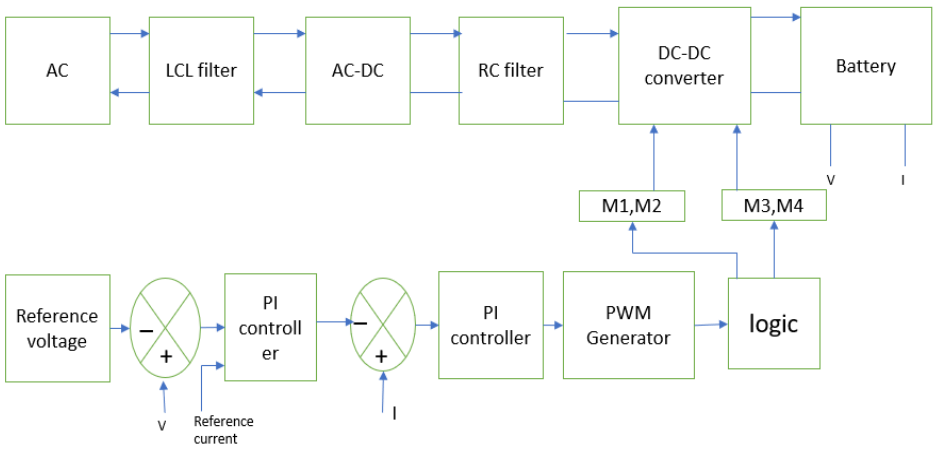

Fig. 1. Block diagram of the proposed system

2 Analysis of The Proposed Converter in Steady State

In the proposed converter the power will be deliver to the load by single phase AC voltage source. The LCL filter is connected next to the input source to reduce total harmonic distortion and maintain power factor. The power flow in the AC-DC system will be assisted by the diodes five and six. The rippled DC has been obtained as the output from the linear transformer. Therefore RC3, RC4 are used to mitigate these ripples (DC). According to the load requirement the battery output voltage has been assisted by the MOSFETS (M1, M2,

M3, M4). The dc flow is maintained in part by the additional diodes (D1, D2, D3, D4). Passive elements like inductor one and two, capacitor (C1) are helpful for filtering and storing purpose. The Lithium-ion battery eventually used as a load.

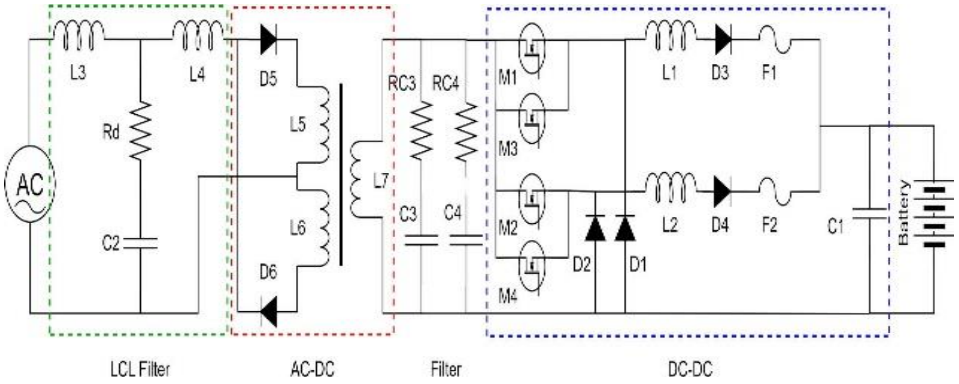

Fig. 2. Circuit Diagram of the converter

3 AC-DC System

There are two different modes of operations in single phase AC voltage source as it changes the phase of the system.

Mode 1:

This mode would occur at 0◦-180◦ supply voltage, with inductors (L3, L4, L5) and Diode D5 are in operating mode and Diode D6 in non-conduction mode producing voltage at inductor 7 which is positive.

Mode 2:

This mode would occur at 180◦–360◦ supply voltage, with inductors L6, L3, L4, and Diode D6 are in operating mode and Diode D5 in non-conduction mode, which again produces a voltage at inductor 7 which is positive.

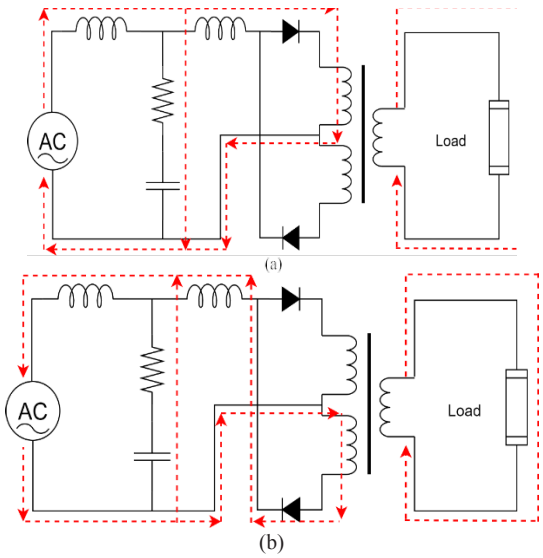

Fig. 3. a&b. Operation modes of AC-DC system

4 Implementation of LCL filter

Resonant frequency of the LCL filter

$$F=\frac{1}{(2\times\pi\times\sqrt{L3\times L4\times C2}\div(L3+L4))}$$

Damping resistance of the filter

$$R=\frac{1}{6\times\pi\times F\times c2}$$

The frequency response of the LCL filter based on transfer function.

$$Y(s)=\frac{1}{(L3\times L4\times C2s^3+(L3+L4)\times C2s^2+(L3+L4)S}$$

Following the aforementioned equations manipulation, the bode plot of LCL filter has been calculated

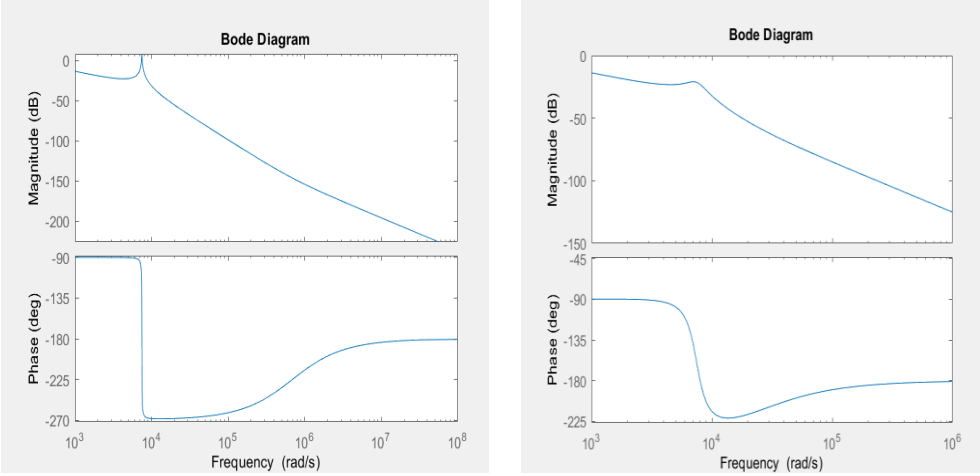

(a) (b)

Fig. 4. a&b. Bode plot for LCL filter

a) with damping resistor
b) without damping resistor

The stability and the intended filter frequency response are implicated in the figure. As a result, the integrated damping resistor shows greater stability in the designed filter.

5 DC-DC Converter

For this analysis, it is assumed that every component is ideal. In addition, the duty cycle and switching frequency have been thought to be fixed. We are doing an open-loop continuous conduction mode analysis of the system. Four modes of the proposed DC-DC converter have been discussed here.

Mode 1: In mode 1 ,0 < t < DTs is the analysis period for the converter. MOSFETs 1 and 2 are currently operating in the conduction mode, while MOSFETs 3 and 4 as well as diodes 1 and 2 are operating in the non-conduction mode. As seen in Figure 4(a), The input source on the left side of the figure is now connected to inductors 1 and 2.

Mode 2: In mode 2, DTs < t < Ts is the analysis period of the converter. Four MOSFETs (M1, M2, M3, M4) are not conducting this time. The conduction mode is now active on diodes 1 and 2. As seen in Figure 4b, inductors L1 and L2 left sides are attached to the ground.
Mode 3: In mode 3, Ts < t < 2DTs is the analysis period for the converter. MOSFETs M3 and M4 are currently operating in the conduction mode, while MOSFETs 3 and 4 as well as diodes 1 and 2 are operating in the non-conduction mode. As seen in Figure 4(c), The input source on the left side of the figure is now connected to inductors L1 and L2.
Mode 4: In mode 4, 2DTs < t < 2Ts is the analysis period of the converter. Four MOSFETs are not conducting this time. The conduction mode is now active on diodes 1 and 2. As seen in Figure 4d, inductors 1 and 2 left sides are attached to the ground.

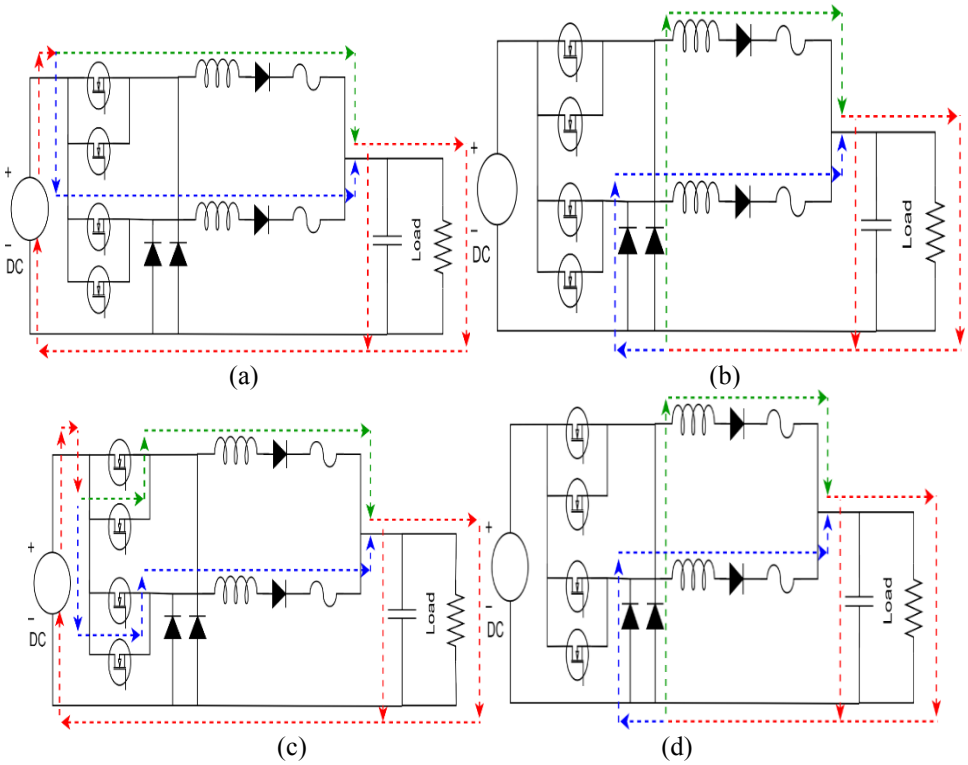

Fig. 5. a, b, c, d. Operation modes of DC-DC converter

Table 1. Parameters of the proposed converter

Components	Specifications
Input voltage source Battery Output voltage Battery Output current	AC Voltage source 56 Volts 153.2 Amps
Output Capacitor	300uF
Inductors (l1, l2)	0.2mH
Inductors (l3, l4)	2.47mH
Switching Capacitor	32kHz
LCL filter capacitor	14.7uF
RC filter capacitor	100uF

6 Simulation Analysis

From the above simulated wave forms we can observe that in less than a second, the average charging current was reached up to about 154A, the SOC went from 60% to 60.04%, conveying to 100% charge. About 17 minutes would be needed to charge the device; that is, 0.04 in one second, 0.08 in two seconds, and so forth. The lithium-ion battery voltage is maintained at approximately 56 volts while it is being charged. Figure 4.2.4 shows the results of a comparison between the suggested control system and the traditional PI. According to the graph, the suggested control system computes faster than the conventional PI because the steady state will be reached in 95.68% less time.

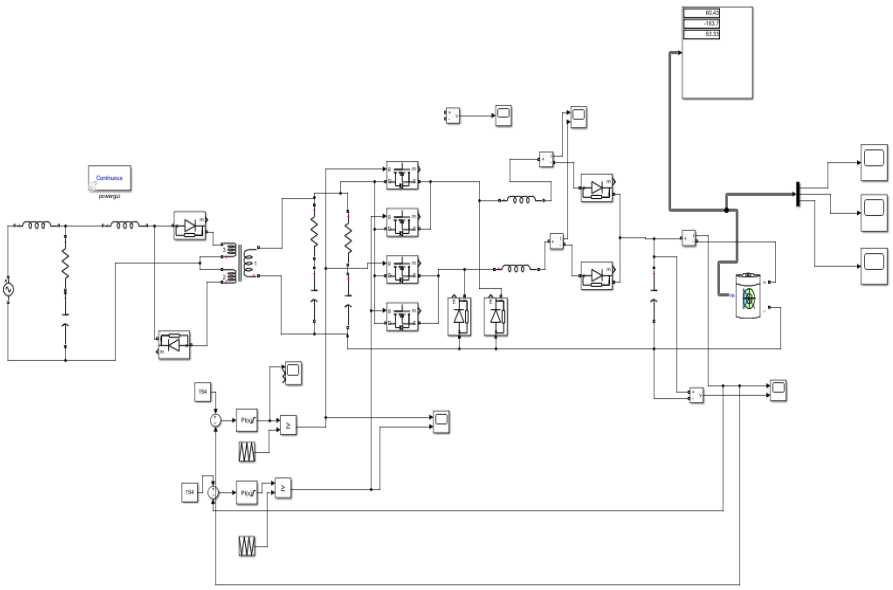

Fig. 6. Simulink diagram of proposed converter

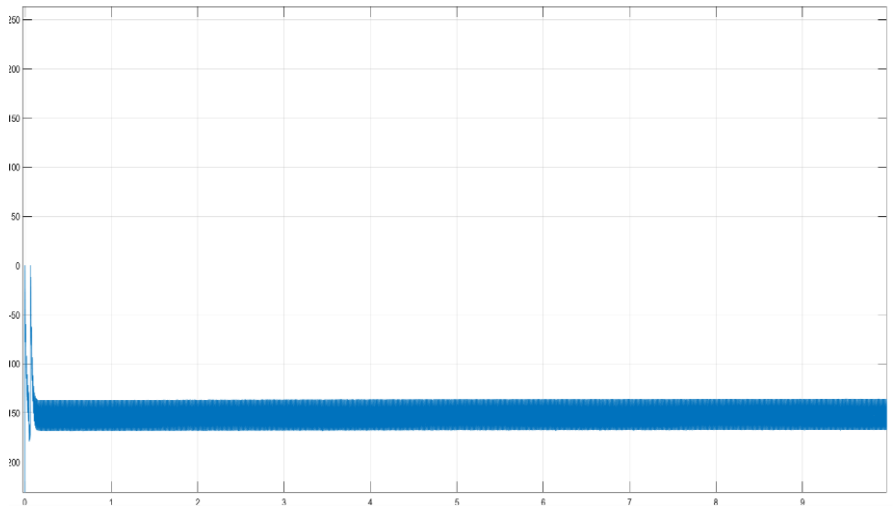

Fig. 7. Output current of the battery

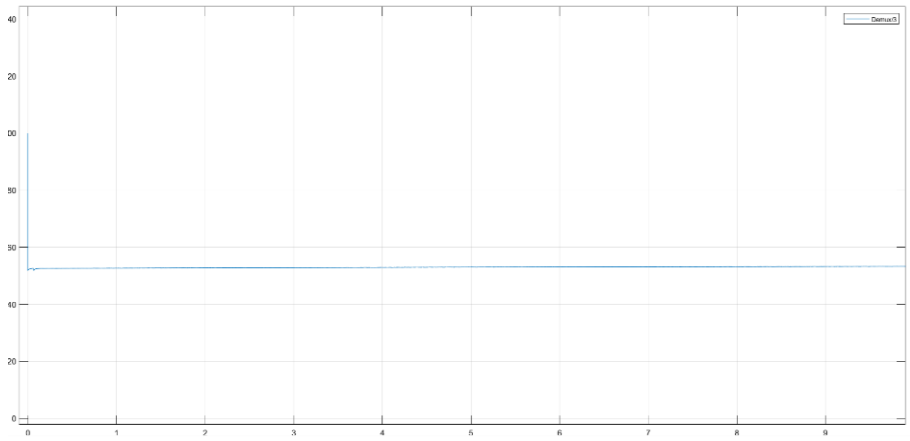

Fig. 8. Output voltage of the battery

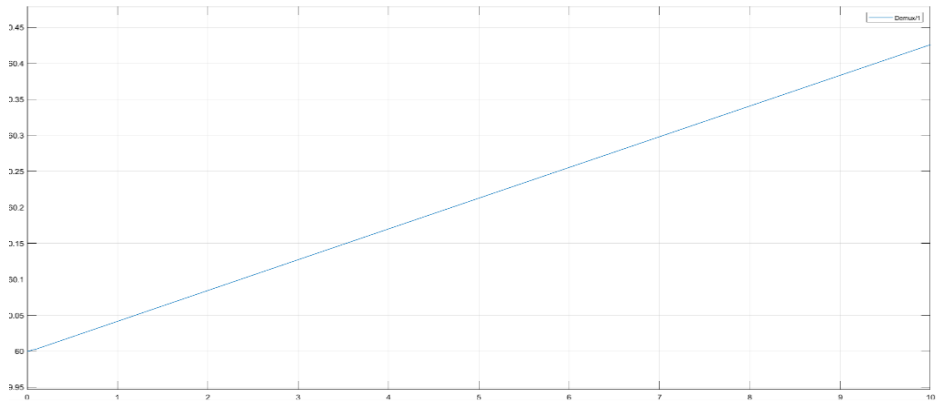

Fig. 9. SOC of the battery

7 Conclusion

The system can maintain negligible overshoot and other factors while charging the lithium-ion battery at 154 Amperes with this type of closed loop high current density converter. Up to approximately 152.1A of charging current was obtained, and the current takes 0.25 seconds to get into steady state. The voltage of the lithium-ion battery was kept at roughly 56V, along with in about a second, the SOC went from 60% to 60.04%, indicating that the battery would take about 17 minutes for 100% charging, meeting the requirements for the two-level fast charging feature. By the end First, a deeper comprehension of converters and their analysis was attained. Second, gained hands-on experience with MATLAB simulation. We were able to analyse the performance of the proposed converter, simulate its behaviour, and see how various parts and parameters responded. We became adept at using MATLAB for circuit simulation through this practical approach.

References

1. M. R. Haque and M. A. Razzak, ‘‘A buck converter-based battery charging controller for electric vehicles using modified PI control system,’’ in Proc. IEEE Int. IoT,

Electron. Mechatronics Conf. (IEMTRONICS), Apr. 2021, pp. 1–4, doi: 10.1109/IEMTRONICS52119.2021.9422646.

2. A. Alassi, A. Al-Aswad, A. Gastli, L. B. Brahim, and A. Massoud, ‘‘Assessment of isolated and non-isolated DC–DC converters for medium voltage PV applications,’’ in Proc. 9th IEEE-GCC Conf. Exhib. (GCCCE), May 2017, pp. 1–6, doi: 10.1109/IEEEGCC.2017.8448079. R. T. Wang, “Title of Chapter,” in *Classic Physiques*, edited by R. B. Hamil (Publisher Name, Publisher City, 1999), pp. 212–213.
3. M. M. Faruk, N. T. Khan, and M. A. Razzak, ‘‘Analysis of the impact of EV charging on THD, power factor and power quality of distribution grid,’’ in Proc. Innov. Power Adv. Comput. Technol. (i-PACT), Nov. 2021, pp. 1–6, doi: 10.1109/i-PACT52855.2021.9697024.
4. M. Su, B. Cheng, Y. Sun, Z. Tang, B. Guo, Y. Yang, F. Blaabjerg, and H. Wang, ‘‘Single-sensor control of LCL-filtered grid-connected inverters,’’ IEEE Access, vol. 7, pp. 38481–38494, 2019, doi: 10.1109/ACCESS.2019.2906239.
5. K. F. I. Faruque, M. R. Uddin, M. I. I. Sakib, and K. M. Salim, ‘‘Mul- tiple outputs converter design for BMS integrated Li-ion battery charger appropriate for electric vehicle,’’ in *Proc. Int. Conf. Sci. Contemp. Technol.(ICSCT)*, Aug. 2021, pp. 1–5, doi: 10.1109/ICSCT53883.2021.9642568.
6. L. Sarker, M. Nazir, and M. A. Razzak, ‘‘Harmonics reduction and power factor correction for electric vehicle charging system,’’ in *Proc. Innov. Power Adv. Comput. Technol. (i-PACT)*, Nov. 2021, pp. 1–6, doi: 10.1109/i-PACT52855.2021.9696738.
7. S. S. Sayed and A. M. Massoud, ‘‘Review on state-of-the-art unidirectional non-isolated power factor correction converters for short-/long-distance electric vehicles,’’ IEEE Access, vol. 10, pp. 11308–11340, 2022, doi: 10.1109/ACCESS.2022.3146410.
8. S. Das, M. R. Haque, and M. A. Razzak, ‘‘Development of one-kilowatt capacity single phase pure sine wave off-grid PV inverter,’’ in Proc. IEEE Region Symp. (TENSYMP), Jun. 2020, pp. 774–777, doi: 10.1109/ TENSYMP50017.2020.9230909.
9. R. N. Beres, X. Wang, F. Blaabjerg, M. Liserre, and C. L. Bak, ‘‘Optimal design of high-order passive-damped filters for grid-connected applications,’’ IEEE Trans. Power Electron., vol. 31, no. 4, pp. 2083–2098, Mar. 2016, doi: 10.1109/TPEL.2015.2441299.
10. (1991). Military Handbook MIL HDBK 217F: Reliability Prediction of Electronic Equipment. USA Department of Defense. Washington, DC, USA.
11. F. Zheng and W. Zhang, ‘‘Long term effect of power factor correction on the industrial load: A case study,’’ in Proc. Australas. Universities Power Eng. Conf. (AUPEC), Nov. 2017, pp. 1–5, doi: 10.1109/AUPEC.2017.8282382.